DNA virus BdDV-1 of the amphibian pathogen *Batrachochytrium dendrobatidis* is associated with hypervirulence

Rebecca Clemons[1] ^, Mark Yacoub[2] ^, Evelyn Faust[1], L. Felipe Toledo[3], Thomas S. Jenkinson[4], Erik Kalinka[5], Lillian K. Fritz-Laylin[5], Timothy Y. James[1] *, Jason E. Stajich[2] *

1. Department of Ecology and Evolutionary Biology, University of Michigan, Ann Arbor, MI 48109, USA
2. Department of Microbiology and Plant Pathology, University of California Riverside, Riverside, CA 92521, USA
3. Laboratório de História Natural de Anfíbios Brasileiros (LaHNAB), Departamento de Biologia Animal Instituto de Biologia (IB), Universidade Estadual de Campinas, Campinas, SP, 13083-862, Brazil
4. Department of Biological Sciences, California State University, East Bay, Hayward, CA 94592, USA
5. Department of Biology, University of Massachusetts Amherst, Amherst, MA 01003 USA

^ Co-First author

* Corresponding authors: Timothy James tyjames@umich.edu, Jason Stajich jason.stajich@ucr.edu

Abstract

The Global Panzootic Lineage (GPL) of the pathogenic fungus *Batrachochytrium dendrobatidis* (*Bd*) has caused severe amphibian population declines, yet the drivers underlying the high frequency of GPL in regions of amphibian decline are unclear. Using publicly available *Bd* genome sequences, we identified multiple non-GPL *Bd* isolates that contain a circular Rep-encoding single stranded DNA-like virus which we named BdDV-1. We further sequenced and constructed genome assemblies with long read sequences to find that the virus is likely integrated into the nuclear genome. Attempts to cure virus positive isolates were unsuccessful, however, phenotypic differences between naturally virus positive and virus negative *Bd* isolates suggested that BdDV-1 decreases the growth of its host *in vitro* but increases the virulence of its host *in vivo*. BdDV-1 is the first described CRESS DNA mycovirus to increase host virulence with a distribution inversely associated with the emergence of the panzootic lineage.

Main

Recent observations of the decline in global amphibian diversity coincide with population genetic evidence of the global spread and emergence of the fungal pathogen *Batrachochytrium dendrobatidis* (*Bd*)[1–4]. In particular, most parasite driven amphibian declines are attributed to the invasion of a low diversity, rapidly expanded Global Panzootic Lineage of *Bd* (*Bd*-GPL)[4–6]. Other *Bd* lineages are mostly enzootic to limited geographic regions and generally do not cause the same large amphibian declines as has been observed with *Bd*-GPL[5,7,8]. Yet, the drivers of relative virulence within and between *Bd* lineages are currently unknown. In other emergent fungal diseases, escape from natural enemies, such as hyperparasitic viruses or other fungi, has been observed and attributed to recent increased transmission or virulence[9,10]. However, no such enemies of *Bd* have been found to date. Here we describe the discovery of a novel DNA mycovirus of *Bd* recovered almost exclusively from the less virulent non-GPL *Bd* lineages.

Mycoviruses, which most commonly have a dsRNA genome, are common hyperparasites of fungi and are known to impact host fitness and virulence[11,12]. Perhaps the most famous example of a mycovirus that impacts host virulence is CHV1, which infects the agent of chestnut blight, *Cryphonectria parasitica*. CHV1 reduces the virulence of its host and has been used with limited success as a biocontrol agent against chestnut blight in some parts of Europe[13]. Previous attempts to screen *Bd* isolates for the presence of dsRNA mycoviruses have yielded negative results[14,15]. Recently, mycoviruses with small ssDNA genomes related to Circular Rep-Encoding Single Stranded (CRESS) DNA viruses have been described from Ascomycete fungi and shown to have a negative impact on host virulence[16–18]. This demonstration that CRESS viruses are more common than appreciated in fungi[19] prompted us to screen for similar mycoviruses in *Bd.* Upon the discovery of such a virus in multiple isolates, we tested for the potential impact of these viruses on fungal phenotypes including virulence towards a model amphibian host.

Results

Viral Discovery

To test how common CRESS viruses are in *Batrachochytrium*, we screened publicly available *Bd* genome sequences from all available lineages[4,5,20] for DNA mycoviruses by *de novo* assembling reads that did not align to the reference genome JEL423. We found that numerous isolates contain viral genes — Rep, encoding a replication-associated protein and Cap, encoding a capsid protein — indicative of a CRESS DNA mycovirus infection. These virus positive isolates almost exclusively within less virulent enzootic *Bd* lineages (**Figure 1A**): Despite being the most sampled lineage only 1 out of 211 sequences of *Bd*-GPL had matches to viral genes (**Figure 1A**). The enzootic *Bd*-BRAZIL lineage is distinctive because less than half of the genome data from these isolates are positive for the Rep gene. The other enzootic lineages of *Bd*-ASIA1 and *Bd*-CAPE have a higher proportion of isolates with copies of the Rep gene, in some cases up to 100% of screened isolates. Notably, the copy number of the virus relative to the genome average was variable between strains (range 0.08-2.49) and was lower in *Bd*-BRAZIL and *Bd*-CAPE than *Bd*-ASIA1 (**Figure 1B**). Additional DNA and protein sequence searches of available *B. salamandrivorans* genomic data did not identify any CRESS-like viral sequences.

Viral Phylogeny and Assembly

We have named this mycovirus *Batrachochytrium dendrobatidis* DNA Virus 1 (BdDV-1). The viral phylogeny constructed from the Rep protein places BdDV-1 in the family Circoviridae (**Figure 1C**). The BdDV-1 lineage is distinct from other identified Fungal CRESS viruses and has a sister relationship to those recovered from environmental sequencing of water, sewage, or viruses associated with animals. The structure of the BdDV-1 genomes recovered from *Bd* isolates has 3 or 4 Open Reading Frames (ORFs) depending on the strain, including Cap and Rep encoding ORFs that are ubiquitous in other CRESS viruses. Comparing the phylogeny of BdDV-1 with a dendrogram of *Bd* strains shows a general fidelity of the virus between *Bd* lineages (Baker's Congruency = 0.94), although there appears to be little cophylogeny within individual lineages (**Figure 1D**). Interestingly, the *Bd*-GPL strain MAD-FR appears to have acquired its BdDV-1 infection from the *Bd*-CAPE lineage that was introduced into Europe[4,20].

The Illumina-based genome assemblies of the virus produced 2-4 kb linear viral contigs with some direct repeats and overlap in the assembly graph indicative of a possible circular genome (**Suppl. Figures 1A-D**). Using these repeats to circularize the genome suggests a viral genome 2.2 kb in length with a single capsid gene and a replication-associated protein gene **(Suppl. Figure 1C**), however lacking the canonical stem-loop motif associated with a nonanucleotide that is characteristic of CRESS viruses[21]. We tested the circular model using outward-facing primers (inverse PCR). The successful amplification of the viral genome using this strategy is consistent with the presence of a circular form of the virus (**Suppl. Figure 1B**). However, attempts to amplify the circular version of the virus using a modified rolling circle amplification protocol[22] were unsuccessful.

Viral Integration

To test whether BdDV-1 infection impacts the phenotype of its host, as is the case with other DNA mycoviruses[16–18], we attempted to generate a virus-free isolate using antivirals. A paired infected and virus-cured *Bd* isolate would allow for the direct comparison of the effects of BdDV-1 on host fungal phenotypes. We tested 71 single zoosporangia isolations from a virus positive *Bd* isolate (CLFT139) grown in control media, or in presence of the antivirals cycloheximide or ribavirin. As each zoosporangium develops from a single zoospore, a single zoosporangium isolate should derive from a single cell. However, all of these curing attempts were unsuccessful, as determined by a PCR test for the presence of the Rep gene after subculturing.

Due to the inability to clear the virus, the inability to amplify the genome via rolling circle replication, and low coverage of the virus in the genome sequencing data (**Figure 1B**), we tested whether the virus may integrate into the genome by sequencing multiple virus-infected strains using long read Oxford Nanopore Technology (ONT). Our assembled *Bd*-BRAZIL isolate CLFT044 genome contained a 4.405kb locus with the entire BdDV-1 genome integrated adjacent to a rDNA locus in a sub-telomeric region of scaffold_10. The viral locus encodes four putative ORFs, a Cap and Rep gene followed by ORF3 and ORF4 which are homologs of a Rep gene. ORF3 and ORF4 are similar to Rep proteins from other CRESS viruses, but are both phylogenetically distinct from BdDV-1 Rep protein (**Suppl. Figure 2**). Additionally, ORF3 and ORF4 shared nearly 100% sequence similarity with each other indicating they may have originated from a duplication or partial integration event.

The viral genome was integrated into a locus 21.2 kb proximal to the telomere and upstream of a GAG-pre integrase gene (**Figure 2A**). Although the ~1 Mb scaffold where BdDV-1 integrated is shared among *Bd* strains, the 21.1199 kb region between the telomere and BdDV-1 locus was not found in v- strains including the reference genome, JEL423. This subtelomeric region in CLFT044 did not contain any predicted protein coding genes (**Figure 2B)**. PCR targeting the region spanning the rDNA region and the Rep ORF confirmed the same integration locus in multiple virus positive strains.

To further explore the localization of BdDV-1, we designed FISH probes to detect the viral genome, as well as a probe to the actin gene as an endogenous *Bd* gene as a control. We used these probes to localize BdDV-1 and actin genes in both virus negative JEL423 and virus positive CLFT044 (**Figure 3A**). We quantified the number of hybridization signal spots and found that the actin control probe localized to either one or two spots in 58% of JEL423 and 32% of CLFT044 cells, while the BdDV-1 probe localized to only 3% of JEL423 cells but 46% of CLFT044 cells (**Figure 3B**). The vast majority of these localization spots co-localized with nuclear DNA signal. The number of foci and the localization of the BdDV-1 compared to the actin gene are consistent with chromosomal integration of the BdDV-1 virus in CLFT044. The integrated nature of BdDV-1 could explain why attempts to cure the virus have been unsuccessful.

To determine whether BdDV-1 ORFs are expressed, we extracted and sequenced mRNA from the virus positive strain CLFT044 and found RNASeq reads that matched the viral ORFs (**Figure 2C**). The Rep gene was the most transcriptionally active viral gene and more highly expressed than the average expression observed in all *Bd* genes.

Growth Assays of Infected Fungal Host

Because we were unable to generate isogenic virus positive and virus negative isolates, we took advantage of the variation within the *Bd*-BRAZIL lineage to determine how the virus may impact its host. We hypothesized that since the Rep gene was present in primarily less virulent non-GPL lineages, BdDV-1 could reduce the virulence of *Bd* isolates. The *Bd*-BRAZIL lineage contains a mixture of isolates both with and without BdDV-1 as detected in genome sequences and validated by PCR of the Rep gene. We chose 8 phylogenetically distinct isolates of *Bd*-BRAZIL, 4 of which were naturally virus positive and 4 of which were naturally virus negative, and conducted growth and experimental infection assays (**Figure 1B**).

We conducted two experiments to measure *in vitro* growth differences between virus positive (v+) and virus negative (v-) *Bd* isolates. The assays differed only in the total number of isolates and replicates. In both assays, zoospores were harvested from v+ and v- *Bd* isolates and diluted at equal concentrations into fresh media. Optical density (OD) readings were recorded for each isolate and averaged between replicates for the duration of the growth period (**Figure 4A,C**). In both of these assays, the growth rate was not different between v+ (1: M=1.73, SD=0.44, 2: M=0.47, SD=0.25) and v- (1: M=2.37, SD=1.34, 2: M=0.71, SD=0.34) isolates, $t(6)=0.87$, $p=0.416$ and $t(4)=0.95$, $p=0.396$ for assays 1 and 2, respectively (**Figure 4A,B**). However, the efficiency of growth or carrying capacity, measured as the difference between the endpoint OD and initial OD, was higher among v- (1: M=0.19, SD=0.06, M=0.12, SD=0.04) compared to v+ (1: M=0.11, SD=0.02, 2: M=0.08, SD=0.02) isolates for both assays, $t(6)=4.22$, $p<0.001$ and $t(4)=3.33$, $p=0.029$ for assays 1 and 2, respectively (**Figure 4B, D**). These results indicate that BdDV-1 reduces the growth of *Bd in vitro*, as it changes the cell density at carrying capacity.

Experimental Infection of Amphibians

To determine the effects of BdDV-1 on *Bd* virulence we infected Dwarf Clawed frogs (*Hymenochirus boettgeri*). Nine groups of 10 frogs each were individually infected with zoospore suspensions from 4 v+ Bd-BRAZIL isolates, 4 v- *Bd*-BRAZIL isolates, or received no infection as a control. The frogs were monitored daily for mortality and morbidity for the duration of the 60 day experiment. All 40 frogs infected with v+ isolates of *Bd* died of their infections by day 43. In contrast, only 28 of 40 frogs infected with v- isolates of *Bd* died of their infection by the end of the 60 days. All 10 control frogs and 12 of 40 frogs infected with v- isolates of *Bd* survived the experiment (**Figure 5A**). Only one v- *Bd* isolate had 100% mortality. According to a Cox proportional hazards model, frogs infected with v+ isolates had a significantly higher risk of death compared to those infected with v- isolates (HR=6.81, 95% CI 1.74-26.64, $p=0.006$). These results indicate that, contrary to our expectations, BdDV-1 is associated with *increased* virulence of *Bd* isolates.

During the experiment, living frogs were also skin swabbed to monitor *Bd* zoospore load via qPCR on day 10, 30, and 60 post *Bd* exposure. A final skin swab was also taken at the time of death. For living frogs, high early time point zoospore loads correlated to higher probabilities of mortality during the experiment (**Suppl. Figure 3**). Among frogs that succumbed, those infected with v- isolates ($M=2.67\times10^5$, $SD=2.61\times10^5$) had a higher zoospore load at death compared to those infected with v+ isolates ($M=6.42\times10^4$, $SD=6.45\times10^4$), $t(6)=5.07$, $p=0.002$ (**Figure 5B**). The number of zoospores at death was not related to survival time, as individuals

infected with the most virulent v- isolate (CLFT144) had similar mean zoospore loads at death to the least virulent v- isolate (CLFT071). This indicates that v+ *Bd* isolates may be associated with a higher virulence than v- isolates for an equivalent infection burden.

To determine the relationship between viral titer and infection outcome, we monitored the relative number of BdDV-1 copies per infected animal via qPCR on collected skin swabs. We found that viral titer, as measured by the ratio of viral copies to fungal nuclear genome copies, varied over time during the infection. In almost all cases, the ratio of viral copies to fungal nuclear genome copies was less than one, and in many cases this ratio was significantly less than 1. For all 4 v+ *Bd* isolates, the ratio decreased among living frogs from day 10 to day 30 post exposure and was lowest among deceased frogs (**Suppl. Figure 4**). This may indicate that while viral presence is significant for the relative virulence of the isolate, it is not necessarily the accumulation of viral genomes in these isolates that leads to increased virulence. Additionally, while virus to fungus ratios did vary between v+ isolates, this variation does not seem to correlate with the relative virulence of these isolates. Causes and consequences of BdDV-1 variation in apparent titer are unclear and an area needing further work.

Discussion

BdDV-1 is the first full length (containing both Rep and Cap genes) CRESS virus in the Circoviridae known to infect fungi. The cophylogeny and genome sequencing data suggest it has a deep history mirroring the diversification of *Bd* and may use both extrachromosomal and chromosomal transmission. Although genome sequence data had been present for the strains used in these studies for over a decade, the presence of BdDV-1 had been overlooked for two reasons. First, most efforts to study mycoviruses have focused on RNA viruses, but DNA mycoviruses may be more prominent than realized[14,19]. Second, analysis which only maps DNA sequence to a single reference genome limits examination to elements found in the assembly; a pangenome approach for the diverse *Bd* lineages is needed to better describe the total diversity of genetic elements of the chytrid fungus[23,24].

BdDV-1 appears to decrease the growth of its host *in vitro*, but increase the virulence of its host *in vivo*. These seemingly contradictory results have only been observed in at least one other mycovirus system[25] to our knowledge. In most mycovirus infections, effects on *in vitro* growth are correlated with effects on host virulence, with both overall positive and overall negative impacts being described[16,18,26]. Although rare, increased fungal virulence due to mycovirus infection could lead to increased spread and transmission of both host and mycovirus[11,27]. However, *in vitro* growth may not correlate with growth in the wild. It is possible that the culture media used contributes to substrate-specific negative impact of BdDV-1 on its host, as has been described with mycoviruses BbPMV-1 and BbPMV-3[28]. On the other hand, the relatively low zoospore loads observed on deceased frogs infected with v+ isolates may indicate that BdDV-1 negatively impacts *Bd* growth both *in vitro* and *in vivo*. If this is the case, then BdDV-1 must be altering *Bd* phenotype in a way that increases virulence without increasing host growth. This could be through the increased production of virulence factors,

which in *Bd* are hypothesized to include metalloproteases and Crinkler Necrosis (CRN) genes[17,29,30].

The broad pattern of vertical inheritance of BdDV-1 in *Bd* lineages may relate to its integration in the fungal chromosome. Rather than a means of genome replication, the endogenization of CRESS viruses is thought to be “accidentally” mediated by the Rep protein during viral replication in the host nucleus[31]. If BdDV-1 inserted itself in the genome early in the origin of *Bd*, it has been maintained as a non-pseudogenized, expressed pair of relevant genes that appear capable of forming extrachromosomal circular molecules. Although BdDV-1 may be primarily expressed from a chromosomal location and inherited through the fungal DNA, its presence is variable across *Bd*-BRAZIL isolates, and its nuclear location would not limit its ability to cause a profound effect on host phenotype. For example, the hypovirulence caused by CHV1 of *C. parasitica* can be recapitulated by expression from an integrated cDNA version of the virus[32]. Moreover, CRESS and other viruses are capable of maintaining both sequence conservation and gene expression following endogenization[33,34]. Additional studies are underway to develop a transfection system to provide a more controlled environment to test the phenotypic effects of BdDV-1.

The demonstration that *Bd* harbors CRESS viruses opens up the potential for exploiting their unique biology for use in biocontrol of the fungus. CRESS viruses have potential to be used as a form of sprayed biocontrol as the ssDNA viruses may show environmental transmission[16,35]. However, in the case of BdDV-1, our results indicate that the virus may increase rather than decrease fungal virulence, making its application in this area unlikely. Instead, *Bd* may change the paradigm that hyperparasites often increase host virulence to increase their Darwinian fitness[36]. Discovery of CRESS viruses of chytrid fungi invite new opportunities for development of vectors to genetically transform chytrids, a much needed research tool. As only a few CRESS mycoviruses have been characterized, there may be a broader opportunity to gain more insight into viral-host interactions. Before any efforts to undertake viral-base remediation or biocontrol strategies, it is imperative to know more about the distribution and potential impact of BdDV-1 and related viruses across amphibian hosts and their parasites.

In conclusion, we describe a novel CRESS virus discovered in *Bd* that is primarily present in the enzootic lineages, suggesting that defense against or escape from a natural enemy such as BdDV-1 could be related to the emergence of *Bd*-GPL. The deep phylogenetic history of the virus, which is found at an even higher prevalence in CAPE & ASIA1 clades sister to the GPL + Brazil lineages, suggests that the common ancestor of most *Bd* lineages would have been infected by BdDV-1 with losses of the virus common in the *Bd*-BRAZIL lineage and before the global dispersal of *Bd*-GPL. By comparing naturally infected *Bd*-BRAZIL isolates with uninfected isolates, we showed the virus causes increased virulence, though the experimental infection and *in vitro* conditions provide only a small snapshot of the true environmental conditions experienced by *Bd*. Importantly, BdDV-1 occurs in the wild in regions in which active hybridization of *Bd* is occurring[4,37]. The threat that hybridization could bring BdDV-1 into a GPL background and increase the virulence of hybrid genotypes is a serious concern. In fact, experimental trials have shown that *Bd* hybrid strains (between *Bd*-GPL and *Bd*-BRAZIL) could be more virulent than parental lineages when infecting native frog hosts[38]. This could have

severe implications for amphibian population declines as viral spillover could increase the virulence of already hypervirulent *Bd* lineages.

Data availability

Genome sequence, annotation for CLFT044 and CLFT071 have been deposited at DDBJ/ENA/GenBank under the accessions JAQIHF000000000, JAQQXB000000000. The version described in this paper is version JAQIHF010000000, JAQQXB010000000. The primary sequence data for Nanopore and Illumina DNA and RNA sequence is deposited under BioProjects PRJNA821523 (CLFT044) and PRJNA913953 (CLFT071). *Bd*-BRAZIL strain sequence data deposited under BioProject PRJNA595972 and NCBI Sequence Read Archive under accessions SRR10698403 (CLFT044), SRR10698397 (CLFT139), SRR10698396 (CLFT148), SRR10698381 (CLFT068), SRR10698424 (CLFT070).

Acknowledgements

LKF-L, TYJ, JES are Fellows in CIFAR program Fungal Kingdom: Threats and Opportunities. The work was partially supported by a catalyst grant from CIFAR and CIFAR fellowship funds. The Gordon and Betty Moore Foundation Award #9337 (10.37807/GBMF9337) to LKF-L, TYJ, JES supported RC, EK, and MY. LKF-L also was supported by a Pew Scholar award from the Pew Charitable Trusts. LFT was granted by the São Paulo Research Foundation (FAPESP #2016/25358-3) and the National Council for Scientific and Technological Development (CNPq #302834/2020-6).

Figure Legends

Figure 1: BdDV-1 is a Circovirus and absent in *Bd*-GPL.
A) Barplot showing percent of infected strains of sampled *Bd* lineages. N indicates the number of isolates with sequenced genomes. **B)** Phylogeny of *Bd* strains constructed from Single Nucleotide Polymorphisms (left) and barplot showing the ratio of Virus to Fungus sequence reads found in each genome sequencing set (right), colored by *Bd* lineage. **C)** A cladogram of the Maximum Likelihood tree estimated from Rep amino acid sequence of BdDV-1 show it as a member of family Circoviridae and distinct from and other mycovirsues (red). Tips are color coded based on viral host and internal numbers represent SH-like support values. **D)** A tanglegram demonstrating co-phylogeny between infected *Bd* strains (left) and BdDV-1 (right). BdDV-1 ML phylogenetic tree constructed based on nucleotide sequences of the Capsid gene. Branch weight indicates common sub-branches between the two trees.

Figure 2: BdDV-1 is integrated into the *Bd* genome and remains transcriptionally active.
A) View of integration supercontigs from 3 BRAZIL strains: v+ strain, CLFT044 (green) and v- strains, CLFT071 (blue) and JEL423 (violet). Shaded linkage shows regions of synteny between the scaffolds. The BdDV-1 integration site is indicated in the CLFT044 scaffold by red shading. **B)** BdDV-1 integration locus in CLFT044 at the end of scaffold 10, including immediate downstream genes (green arrows). Locus IDs in CLFT044 annotation and Functional annotations are indicated. Genes of unknown function are labeled with their highest BLAST hit in reference genomes JEL423 or JAM81. The region spanning the telomere to ~100kb region is not shared between infected and uninfected strains. **C)** BdDV-1 locus structure with log transformed expression at each position indicated using black bars. The average log transformed expression across all *Bd* genes is depicted by the green horizontal line. The Rep gene alone is highly expressed compared to fungal genes.

Figure 3: BdDV-1 genome localization using DNA FISH.
A) Zoospores from v- strain JEL423 and v+ strain CLFT044 were fixed and stained with DNA probes targeting the *Bd* actin locus (left) or a region of the BdDV-1 genome (right). Images show overlays of DNA probe (green) and DAPI (magenta) fluorescence, dashed lines indicate cell boundaries and flagella. The brightness and contrast of probe signal were increased in actin/CLF044 image to improve visibility of foci. Scale bars: 5 µm. **B)** Quantification of hybridization signal spots per cell. Numbers of cells analyzed are indicated in parentheses.

Figure 4: *Bd* isolates naturally infected with BdDV-1 (v+) show reduced growth efficiency compared to virus-free strains (v-).

A, C) Two independent growth curves are shown for infected (v+, green) and uninfected (v-, purple) strainsGray shading indicates the 95% confidence interval. **B, D**) Comparisons of averages between all v- and v+ isolates for efficiency of growth (EOG) and rate of growth for

first assay (**B**) and second assay (**D**). * indicates a significant difference between groups (p<.05). Error bars represent 95% confidence intervals.

Figure 5: **Frogs infected with v+ isolates have higher mortality rates but lower zoospore loads at death.**
A) Frog host survival for the 60 day experimental infection. Frogs infected with virus positive *Bd* strains (green) have a higher chance of mortality compared to frogs infected with virus negative *Bd* strains (purple). There was no mortality in the control group (gray). **B)** qPCR data showing the zoospore quantity at time of death for all frogs that died during the experiment. Frogs infected with virus negative strains (purple) had higher zoospore loads at death.

Supplemental Figure 1: **BdDV-1 genome structure and PCR confirmation of its presence among *Bd* isolates. A)** Dot plot of NODE 611 of Illumina based assembly of the BdDV-1 virus in CLFT044. The presence of direct repeats suggested a possible circular structure of the genome. The pink area was extracted for a circularized version. **B)** Genome structure of circular version of BdDV-1 from CLFT044. Primers are shown as small arrows indicating which strand they represent. The nonanucleotide motif present (GAATATTAA) as identified by sl-finder notably is lacking a supporting stem-loop structure. **C)** Amplification of overlapping primers is consistent with presence of a circular form of BdDV-1 in four Bd v+ strains. Four v+ strains (CLFT148, CLFT061, CLFT044, CLFT067), 3 v- strains (CLFT144, CLFT068, CLFT071), and a water control were amplified with the primer pairs shown in that respective order. Samples (3 ul) were loaded in between lanes of DNA ladder. **D)** Assembly graph of regions of the Illumina-based assembly of CLFT044 that contain sequence matching NODE 611. Four contigs (arrows) form a loop that is consistent with a circular version of the genome. Assembly graph was visualized using the tool *bandage*.

Supplemental Figure 2: Phylogram of the Rep gene from CRESS viruses. Phylogeny shows the relationships of the CRESS viruses based on the Rep protein. The BdDV-1 integrated locus also encodes two ORFs (ORF3 and ORF4 drawn in Red) which are homologous to the Rep protein and their position and relationships to other CRESS Rep sequences.

Supplemental Figure 3: **qPCR data showing the zoospore quantification from surviving frogs.** Frogs infected with virus negative strains of *Bd* are indicated in purple, frogs infected with virus positive strains of Bd are indicated in green, and control frogs are indicated in gray. Missing data for day 30 or day 60 means that all the frogs from that group had succumbed before that time point.

Supplemental Figure 4: qPCR data showing ratio of BdDV-1 copies to *Bd* zoospores (genomic equivalents) decreases over the infection period.

Supplemental Table 1: *Bd* isolates used in this study presenting collection information and viral presence.

Supplemental Table 2: Primer and probe sequences used for viral presence confirmation, viral circularity confirmation, DNA FISH, viral integration confirmation, and viral qPCR

Supplemental Table 3: *Bd* strains from public Sequence Read Archive records used for screening of viral presence.

Online Methods

Viral discovery from screening Bd sequencing reads

Published isolate DNA sequence Illumina reads were downloaded from the National Center for Biotechnology Information (NCBI) Sequence Read Archive (SRA) (**Suppl. Table S3**). Illumina sequence reads were aligned to the *Bd* JEL423 genome with bwa v0.7.17[39] and processed with samtools to identify those reads which did not align to the genome (samtools fastq -f 4 BAMFILE). These reads were further assembled with SPAdes v3.15.2[40]. The resulting contigs were screened by translated searches against UniProt databases which identified regions of assembled contigs as homologous to viral Rep genes. The ORFs were further predicted from the contig assembly with prodigal v2.6.3[41].

CRESS Rep Phylogeny

Virus Rep proteins from representatives of the major families of CRESS viruses (Geminiviridae, Genomoviridae, Circoviridae) were obtained from the UniProt database. The Rep proteins from these viruses and BdDV-1 were aligned with MUSCLE v5.1[42], and a phylogeny was constructed with IQTREE v2.2.1[43]. Software scripts for these analyses are archived at github https://github.com/myacoub005/CRESS_Phylogeny.

Strain Phylogeny

A phylogeny of the Bd strains was constructed from raw alignments of the reads to JEL423 genome following GATK best practices and assuming diploid genomes. A NJ phylogenetic tree of the strains constructed with Poppr[44]. Software and scripts to run the variant calling, mapping of reads, detection of unmapped reads, and tree construction are archived in https://github.com/stajichlab/PopGenomics_Bd.

BdDV-1 Tanglegram

The Cap nucleotide sequences from the Illumina genomes were aligned using MUSCLE v5.1 and the phylogeny was constructed with IQTREE v2.2.1[43]. A tanglegram was constructed against the *Bd* strain phylogeny using the R package dendextend[45].

Illumina assembly of strain CLFT044

The genomes of strain CLFT044 and additional *Bd*-BRAZIL strains were sequenced using paired-end (2x125 bp) sequencing on an Illumina NextSeq HiSeq-2500 v4 platform. Reads were trimmed for adapters and quality using *Trimmomatic*[46] and *de novo* assembled with *SPAdes v3.15.5*[40]. After identification of a single contig of 3,647 bp that contained blast matches to the Rep gene, the putative viral contig was compared to itself using the BLAST algorithm implemented in *YASS*[47]. We also inspected the assembly graph produced by *spades* for evidence of loops indicating circularity using the software *Bandage*[48].

RNA Extraction and Sequencing of CLFT044

RNA was extracted from 7 day old cultures of CLFT044 and CLFT071 grown on 1% Tryptone Agar at 18*C using TRIzol following manufacturer's instructions and incorporating a 12 hour isopropanol precipitation to increase yields. Total RNA was sent to *Novogene* for polyA enrichment and NovaSeq PE150 sequencing to obtain 6G raw data per sample. Reads were aligned to the assembled CLFT044 genome using bwa v0.7.17[39] to determine transcriptional activity of BdDV-1.

Nanopore assembly and annotation of *Bd*-BRAZIL Strains CLFT044 and CLFT071

Tissue was collected from 7 day old cultures of CLFT044 and CLFT071 grown on 1% Tryptone Agar at 21 C by flooding plates with 1 mL of sterile RO water, scraping colonies with an L-spreader, and collecting into a 2 mL sterile tube. Tubes were centrifuged at 6500 rcf to remove supernatant and flash frozen with liquid nitrogen. DNA was extracted from tissue using a Cetyltrimethylammonium Bromide (CTAB) extraction protocol[49]. The DNA was sent to MiGS (now SeqCenter) to obtain 900 Mb (~30X coverage) of Oxford Nanopore sequence reads for CLFT044 and CLFT071. The reads were *de novo* assembled using *Canu* v2.2[50] followed by 10 iterations of polishing with *Pilon* v1.24[51] with *Illumina* sequence data. Annotation was performed using Funnanotate v1.8.14[52] which trained gene predictors on RNAseq data to improve annotation accuracy.

Identification of the Viral Locus

The BdDV-1 locus was identified through BLAST v2.13 searches using the viral Rep gene obtained from the Illumina *Bd* genomes against the CLFT044 ONT genome annotation. The raw Illumina FASTQ data from v+ and v- strains were aligned against the CLFT044 ONT genome using bwa v0.7.17[39] to identify the full length 4.405kb region that makes up BdDV-1. This region was covered only by v+ strains and absent in all v- strains. The 4 proteins in this region were searched against the UniProt and NCBI databases to confirm they were viral in origin.

Culture Acquisition

All *Bd* isolates are deposited in CZEUM (Collection of Zoosporic Eufungi at the University of Michigan)[53] and maintained on 1% tryptone (1%T) growth medium. All isolates used belong to the non-GPL *Bd*-BRAZIL lineage and were genetically characterized[54]. Five isolates were determined to be virus positive though genome sequence analysis (CLFT061, CLFT067, CLFT044, CLFT148, CLFT139), and four additional isolates were determined to be virus negative (CLFT068, CLFT070, CLFT071, CLFT144).

Confirmation of Viral Presence and Circularity

Viral presence was confirmed using PCR with BdDV-1 specific primers to amplify a 591 bp fragment. The circularity of the virus was confirmed on a subset of samples by using 2 BdDV-1 specific primer sets that were reverse complements of one another. One primer set amplified a ~800 bp region, and the other set amplified the remaining ~1400 bp of the 2.2kb circular viral genome. See Supp. table 2 for primer sequences. All PCR reactions followed the manufacturer recommended recipe for Phusion High Fidelity Polymerase (New England

BioLabs, Inc.) with these PCR conditions: 98 °C 30 s, 40 cycles (98 °C 10 s, 60 °C 20 s, 72 °C 30 s), 72 °C 7 min.

Rolling circle amplification (RCA) was attempted on a subset of samples that were confirmed to be virus positive through PCR testing. A TempliPhi 100 Amplification Kit (Cytiva) was used, following a slightly modified protocol[22]. BdV-2F and BdV-3R PCR primers were added to the reaction to target BdDV-1. RCA products were digested with a *Sca*I restriction enzyme (Thermo Fisher Scientific) following manufacturer instructions.

Fluorescence in situ hybridization (FISH)

Probe synthesis and labeling

Polynucleotides were synthesized by PCR using Phusion High-Fidelity DNA polymerase (NEB, M0530L) and locus-specific primers (see **Suppl. Table 2** for sequences). To target the BdDV-1 genome, a 2143 bp region was amplified from CLFT044 total DNA. For the *Bd* actin locus, a 2058 bp probe was synthesized from JEL423 total DNA.

Following spin column purification (Macherey-Nagel, 740609), the PCR products were directly labeled with Alexa Fluor 555 dye and purified using the FISH Tag DNA Orange Kit (ThermoFisher Scientific, F32948). Labeling was performed according to the manufacturer's instructions, with the following modification: 0.95 µL DNase I working solution and 1.2 µg of template DNA were used in the nick translation reaction. Labeled probe concentrations were determined spectrophotometrically using a NanoDrop 2000 (Thermo Scientific).

Cell fixation and staining

Bd strains JEL423 and CLFT044 were grown in 1% tryptone (w/v) at 24 °C in tissue culture-treated flasks (Fisher, 50-202-081), washed once and resuspended in Bonner's salts (10.27 mM NaCl, 10.06 mM KCl, 2.7 mM $CaCl_2$ in MilliQ water) to a final concentration of $1x10^7$ zoospores/mL. 96-well glass bottom plates (Eppendorf, EP0030741030) were plasma cleaned, immediately coated with a 1 mg/mL Concanavalin A (Sigma, C2010) solution for 8 min, washed thrice with Bonner's salts, and overlaid with 120 µL of the resuspended *Bd* zoospores. Cells were allowed to adhere to the Concanavalin A for 5 min before fixation with 200 µL of 4% paraformaldehyde in 50 mM cacodylate buffer (pH 7.2). Cells were fixed on ice for 20 min, then for 10 min at room temperature before being washed three times with PBS (137 mM NaCl, 2.7 mM KCl, 10 mM Na_2HPO_4, 1.8 mM KH_2PO_4) for 5 min. Samples were then permeabilized in 0.2 % Triton X-100 in PBS for 12 min at room temperature (about 23 °C) and washed thrice with PBS.

Cells were then rinsed once with prehybridization buffer (50 % deionized formamide [Invitrogen, AM9342], 2xSSC [0.3 M NaCl, 0.03 M sodium citrate, pH 7.0], 10 % dextran sulfate [Sigma-Aldrich,D8906]). 75 µL prehybridization buffer was then added to each well, the plate was sealed with adhesive aluminum foil and incubated for 30 min at 37 °C and subsequently transferred to a preheated lab oven set at 85 °C for 12.5 min to denature cellular DNA. During this time, FISH probes were prepared by diluting labeled probes in prehybridization buffer to a

final concentration of 1.5 ng/µL,denatured at 93 °C for 5 min, placed on ice for 1 min, and then kept at room temperature (about 25 °C).

Following oven incubation, the 96 well plate was briefly centrifuged, the prehybridization buffer was gently aspirated with a micropipette and 75 µL denatured probe mix was added to each well. Immediately afterwards, the plate was resealed, moved to a humid hybridization chamber, and incubated for 38-42 h at 37 °C. Unbound probes were removed by low-stringency washes at room temperature. Specifically, cells were rinsed briefly once with 2xSSC, twice for 5 min in 2xSSC, twice in 0.4xSSC for 5 min,once for 5 min in 4xSSC,twice in PBS and then counterstained with 1µg/mL DAPI in PBS for 10 min, rinsed twice with PBS, and then overlaid with PBS for imaging.

Microscopy and image analysis

Cells were imaged on a Nikon Ti2-E inverted microscope equipped with a 100x oil PlanApo objective and sCMOS 4mp camera (PCO Panda). Images were acquired at room temperature using both DIC microscopy, and epifluorescence microscopy with excitation light at 400 nm to visualize DAPI and 550 nm to visualize the Alexa Fluor 555 dye-conjugated probes. Images were further processed in Fiji[55]. The number of hybridization signal spots per cell was determined from overlays of DAPI and FISH probe micrographs by manual counting. A total of 4-9 pictures were analyzed for each sample. Final micrographs for Figure 1E were composed in Inkscape (Inkscape Project, 2020).

Confirmation of Viral Integration

Viral integration was confirmed using PCR primers to amplify the 1023bp region spanning the right flank of the integration locus: Rep gene (BdVlf-F) to *Bd* ITS1_SSU region (BdVlf-R). See **Suppl. Table 2** for primer sequences.

Curing Attempts

Virus positive isolates were streaked onto 1% tryptone plates. After 3-4 days of growth single zoosporangia were isolated onto fresh 1%T plates with a sterile wire tool. The virus positive isolates were also grown on 0.1 mg/L cycloheximide 1%T plates. After streaking, cultures onto media with cycloheximide, single zoosporangia were transferred to fresh 0.1 mg/L cycloheximide 1%T plates. After 3-4 days of growth, single zoosporangia were isolated to fresh 1%T plates. The same method was used with 80 µM ribavirin instead of cycloheximide. All of the single zoosporangia isolations were allowed to grow to saturation then tested for viral presence by PCR.

Growth Assay

Four virus positive and four virus negative isolates were grown independently on 1%T plates. After 7 days, each plate was flooded with 2 mL of liquid 1%T media and left to incubate at room temperature for 30 min. Zoospores were then harvested from each plate. The zoospore concentration of each isolate was estimated using a Multisizer 4e Coulter Counter (Beckman Coulter, Inc.).

For the first assay, each isolate was diluted into 1 mL of liquid 1%T media at a concentration of 10^6 zoospores/mL in a 24-well plate with 2 replicates per isolate. The isolates

were allowed to grow at room temperature for 5 days, and the optical density (OD) was recorded every hour using a Epoch 2 Microplate Spectrophotometer (BioTek Instruments).

For the second assay, zoospore dilutions were prepared as described above, except in a total volume of 0.8 mL 1%T media in a 48-well plate with 5 replicates per isolate. Only 6 of the isolates were used (3 virus positive and 3 virus negative). The lid of the plate was treated with Triton X-100[56] to prevent condensation on the underside of the lid. The isolates were allowed to grow for 12 days with an OD measurement every hour. The plates were agitated by gentle shaking for 5 seconds before each OD measurement. For both assays, efficiency of growth was measured as the difference between the average OD at the final three time points and the average OD at the first three time points. The growth rate was determined using the means of the highest positive slopes during the growth period[57]. For each assay, a nested t-test was performed to determine differences in the efficiency of growth or growth rate between virus positive and virus negative isolates.

Experimental Infection

We performed all investigations involving live vertebrate animals following protocols approved by the University of Michigan Institutional Animal Care and Use Committee (IACUC protocol PRO00009614). Dwarf Clawed frogs (*Hymenochirus boettgeri*) were acquired from vendors Live Aquaria and VWR. Upon arrival, the frogs were group-housed in 37 liter aquaria at a maximum of 20 frogs per tank. After a 3-5 day acclimation period, the frogs were heat treated to remove any incoming *Bd* infection following previous work[58]. The tank temperature was raised 1 °C per day until reaching a maximum temperature of 30 °C. The tanks were maintained at 30 °C for 7 days, and then lowered by 1 °C per day until returning to 21 °C ambient room temperature.

To prepare inoculum, zoospores were harvested and concentrations estimated for each of the 8 *Bd* isolates as described above for the growth assays. However, instead of flooding with liquid 1%T media, plates were flooded instead with sterile water. The zoospore suspensions were diluted to a concentration of 2.5×10^5 zoospores/mL in autoclave sterilized RO water with aquarium salt. 10 mL of each suspension were aliquoted into sterile 50 ml conical tubes.

Post-heat treatment, 90 frogs were chosen at random and sorted into randomized experimental groups with 10 frogs per group. Each frog was weighed as a proxy for body size, and then immediately placed in an individual 50 mL tube with the zoospore suspension. Ten frogs were placed into 50 mL tubes with *Bd*-free autoclave sterilized RO water with aquarium salt as a control group. The frogs remained in the tubes for a 6 hour inoculation, then the frog and the entire zoospore suspension were added to individual 0.9 L aquaria.

The frogs were housed and cared for in the individual aquaria for the remainder of the 60 day experiment with daily monitoring for mortality and morbidity. Frogs were removed from the tanks and swabbed using Medical Wire & Equipment fine tip rayon swabs at day 10, day 30, day 60, and at death or euthanasia. Swabs were DNA extracted using a DNeasy blood and tissue kit (Qiagen). Living frogs were weighed at day 30 and day 60 to estimate health and body condition. A Cox proportional hazards model, clustered by isolate, was used to determine

differences in hazard ratios between v+ and v- infected frogs. A Spearman correlation test was performed to determine if initial body weight influenced the probability of survival of *Bd*-infected frogs.

qPCR for *Bd* Zoospore Equivalents and BdDV-1 viral copies

Real-time quantitative PCR was performed on DNA extracted swabs to determine *Bd* zoospore equivalents[59]. Swabs from control frogs and frogs infected with virus negative isolates of *Bd* were single-plexed using only a *Bd* specific qPCR assay. Swabs from frogs infected with virus positive isolates of *Bd* were multiplexed using both a *Bd* specific assay and a BdDV-1 specific assay. See Supp. table 2 for primer and probe sequences. Standards for viral copy number were created by cloning PCR product using custom BdDV-1 primers into the pCR 2.1-TOPO vector using the TOPO TA cloning kit (Invitrogen). Transformed *Escherichia coli* colonies with successful insert were plasmid extracted using the Zyppy Plasmid Miniprep kit (Zymo Research). Plasmid copy numbers were estimated using the formula:

Number of copies per µL = [(g/µL) / plasmid length in bp * 650)] * (6.022 * 10^{23})

Ten-fold dilutions of viral standards were created with 10^6 plasmid copies through 10^0 plasmid copies. Ten-fold dilutions of *Bd* standards were created starting with DNA extracted from 10^6 zoospore suspensions. All qPCR reactions were run on a QuantStudio 3 qPCR machine (Applied Biosystems). A nested t-test was performed to determine if there was a difference between average zoospore load on dead frogs infected with virus positive or virus negative *Bd* isolates.

References

1. James, T. Y., Litvintseva, A. P., Vilgalys, R., Morgan, J. A. T., Taylor, J. W., Fisher, M. C., Berger, L., Weldon, C., du Preez, L. & Longcore, J. E. Rapid global expansion of the fungal disease chytridiomycosis into declining and healthy amphibian populations. *PLoS Pathog.* **5,** e1000458 (2009).
2. Fisher, M. C., Garner, T. W. J. & Walker, S. F. Global Emergence of *Batrachochytrius dendrobatidis* and Amphibian Chytridiomycosis in Space, Time, and Host. *Annu. Rev. Microbiol.* **63,** 291–310 (2009).
3. Scheele, B. C., Pasmans, F., Skerratt, L. F., Berger, L., Martel, A., Beukema, W., Acevedo, A. A., Burrowes, P. A., Carvalho, T., Catenazzi, A., De la Riva, I., Fisher, M. C., Flechas, S. V., Foster, C. N., Frías-Álvarez, P., Garner, T. W. J., Gratwicke, B., Guayasamin, J. M., Hirschfeld, M., Kolby, J. E., Kosch, T. A., La Marca, E., Lindenmayer, D. B., Lips, K. R., Longo, A. V., Maneyro, R., McDonald, C. A., Mendelson, J., 3rd, Palacios-Rodriguez, P., Parra-Olea, G., Richards-Zawacki, C. L., Rödel, M.-O., Rovito, S. M., Soto-Azat, C., Toledo, L. F., Voyles, J., Weldon, C., Whitfield, S. M., Wilkinson, M., Zamudio, K. R. & Canessa, S. Amphibian fungal panzootic causes catastrophic and ongoing loss of biodiversity. *Science* **363,** 1459–1463 (2019).
4. O'Hanlon, S. J., Rieux, A., Farrer, R. A., Rosa, G. M., Waldman, B., Bataille, A., Kosch, T. A., Murray, K. A., Brankovics, B., Fumagalli, M., Martin, M. D., Wales, N., Alvarado-Rybak, M., Bates, K. A., Berger, L., Böll, S., Brookes, L., Clare, F., Courtois, E. A., Cunningham, A. A., Doherty-Bone, T. M., Ghosh, P., Gower, D. J., Hintz, W. E., Höglund, J., Jenkinson, T. S., Lin, C.-F., Laurila, A., Loyau, A., Martel, A., Meurling, S., Miaud, C., Minting, P., Pasmans, F., Schmeller, D. S., Schmidt, B. R., Shelton, J. M. G., Skerratt, L. F., Smith, F., Soto-Azat, C., Spagnoletti, M., Tessa, G., Toledo, L. F., Valenzuela-Sánchez, A., Verster, R., Vörös, J., Webb, R. J., Wierzbicki, C., Wombwell, E., Zamudio, K. R., Aanensen, D. M.,

James, T. Y., Gilbert, M. T. P., Weldon, C., Bosch, J., Balloux, F., Garner, T. W. J. & Fisher, M. C. Recent Asian origin of chytrid fungi causing global amphibian declines. *Science* **360,** 621–627 (2018).

5. Rosenblum, E. B., James, T. Y., Zamudio, K. R., Poorten, T. J., Ilut, D., Rodriguez, D., Eastman, J. M., Richards-Hrdlicka, K., Joneson, S., Jenkinson, T. S., Longcore, J. E., Parra Olea, G., Toledo, L. F., Arellano, M. L., Medina, E. M., Restrepo, S., Flechas, S. V., Berger, L., Briggs, C. J. & Stajich, J. E. Complex history of the amphibian-killing chytrid fungus revealed with genome resequencing data. *Proc. Natl. Acad. Sci. U. S. A.* **110,** 9385–9390 (2013).
6. Farrer, R. A., Martel, A., Verbrugghe, E., Abouelleil, A., Ducatelle, R., Longcore, J. E., James, T. Y., Pasmans, F., Fisher, M. C. & Cuomo, C. A. Genomic innovations linked to infection strategies across emerging pathogenic chytrid fungi. *Nat. Commun.* **8,** 14742 (2017).
7. Rodriguez, D., Becker, C. G., Pupin, N. C., Haddad, C. F. B. & Zamudio, K. R. Long-term endemism of two highly divergent lineages of the amphibian-killing fungus in the Atlantic Forest of Brazil. *Mol. Ecol.* **23,** 774–787 (2014).
8. Belasen, A. M., Russell, I. D., Zamudio, K. R. & Bletz, M. C. Endemic lineages of *Batrachochytrium dendrobatidis* are associated with reduced chytridiomycosis-induced mortality in amphibians: Evidence from a meta-analysis of experimental infection studies. *Front Vet Sci* **9,** 756686 (2022).
9. Milgroom, M. G. & Cortesi, P. Biological control of chestnut blight with hypovirulence: a critical analysis. *Annu. Rev. Phytopathol.* **42,** 311–338 (2004).
10. Kiss, L. Natural occurrence of *Ampelomyces* intracellular mycoparasites in mycelia of powdery mildew fungi. *New Phytol.* **140,** 709–714 (1998).
11. Parratt, S. R. & Laine, A. L. The role of hyperparasitism in microbial pathogen ecology and evolution. *ISME Journal* **10,** 1815–1822 Preprint at https://doi.org/10.1038/ismej.2015.247

(2016)

12. Kondo, H., Botella, L. & Suzuki, N. Mycovirus Diversity and Evolution Revealed/Inferred from Recent Studies. *Annu. Rev. Phytopathol.* **60,** 307–336 (2022).
13. Rigling, D. & Prospero, S. *Cryphonectria parasitica*, the causal agent of chestnut blight: invasion history, population biology and disease control. *Mol. Plant Pathol.* **19,** 7–20 (2018).
14. Myers, J. M., Bonds, A. E., Clemons, R. A., Thapa, N. A., Simmons, D. R., Carter-House, D., Ortañez, J., Liu, P., Miralles-Durán, A., Desirò, A., Longcore, J. E., Bonito, G., Stajich, J. E., Spatafora, J. W., Chang, Y., Corrochano, L. M., Gryganskyi, A., Grigoriev, I. V. & James, T. Y. Survey of early-diverging lineages of fungi reveals abundant and diverse mycoviruses. *MBio* **11,** e02027–20 (2020).
15. Webb, R. J., Roberts, A. A., Wylie, S., Kosch, T., Toledo, L. F., Merces, M., Skerratt, L. F. & Berger, L. Non-detection of mycoviruses in amphibian chytrid fungus (*Batrachochytrium dendrobatidis*) from Australia. *Fungal Biol.* **126,** 75–81 (2022).
16. Khalifa, M. E. & Macdiarmid, R. M. A Mechanically Transmitted DNA Mycovirus Is Targeted by the Defence Machinery of Its Host, *Botrytis cinerea*. *Viruses* **13,** 1315 (2021).
17. Li, P., Wang, S., Zhang, L., Qiu, D., Zhou, X. & Guo, L. A tripartite ssDNA mycovirus from a plant pathogenic fungus is infectious as cloned DNA and purified virions. *Science Advances* **6,** eaay9634 (2020).
18. Yu, X., Li, B., Fu, Y., Jiang, D., Ghabrial, S. A., Li, G., Peng, Y., Xie, J., Cheng, J., Huang, J. & Yi, X. A geminivirus-related DNA mycovirus that confers hypovirulence to a plant pathogenic fungus. *Proc. Natl. Acad. Sci. U. S. A.* **107,** 8387–8392 (2010).
19. Zhao, L., Lavington, E. & Duffy, S. Truly ubiquitous CRESS DNA viruses scattered across the eukaryotic tree of life. *J. Evol. Biol.* **34,** 1901–1916 (2021).
20. Farrer, R. A., Weinert, L. A., Bielby, J., Garner, T. W. J., Balloux, F., Clare, F., Bosch, J., Cunningham, A. A., Weldon, C., du Preez, L. H., Anderson, L., Pond, S. L. K., Shahar-Golan, R., Henk, D. A. & Fisher, M. C. Multiple emergences of genetically diverse

amphibian-infecting chytrids include a globalized hypervirulent recombinant lineage. *Proc. Natl. Acad. Sci. U. S. A.* **108,** 18732–18736 (2011).

21. Rosario, K., Duffy, S. & Breitbart, M. A field guide to eukaryotic circular single-stranded DNA viruses: insights gained from metagenomics. *Arch. Virol.* **157,** 1851–1871 (2012).
22. James, A. P., Geijskes, R. J., Dale, J. L. & Harding, R. M. Development of a Novel Rolling-Circle Amplification Technique to Detect Banana streak virus that also Discriminates Between Integrated and Episomal Virus Sequences. *Plant Dis.* **95,** 57–62 (2011).
23. Plissonneau, C., Hartmann, F. E. & Croll, D. Pangenome analyses of the wheat pathogen *Zymoseptoria tritici* reveal the structural basis of a highly plastic eukaryotic genome. *BMC Biol.* **16,** 5 (2018).
24. Lofgren, L. A., Ross, B. S., Cramer, R. A. & Stajich, J. E. The pan-genome of *Aspergillus fumigatus* provides a high-resolution view of its population structure revealing high levels of lineage-specific diversity driven by recombination. *PLoS Biol.* **20,** e3001890 (2022).
25. Okada, R., Ichinose, S., Takeshita, K., Urayama, S. I., Fukuhara, T., Komatsu, K., Arie, T., Ishihara, A., Egusa, M., Kodama, M. & Moriyama, H. Molecular characterization of a novel mycovirus in *Alternaria alternata* manifesting two-sided effects: Down-regulation of host growth and up-regulation of host plant pathogenicity. *Virology* **519,** 23–32 (2018).
26. Lima, S. S., Abadio, A. K. R., Araújo, E. F., Kitajima, E. W., Sartorato, A. & De Queiroz, M. V. Mycovirus in *Pseudocercospora griseola*, the causal agent of angular leaf spot in common bean. *Can. J. Microbiol.* **56,** 359–365 (2010).
27. Sandhu, S. K., Morozov, A. Y., Holt, R. D. & Barfield, M. Revisiting the Role of Hyperparasitism in the Evolution of Virulence. *Am. Nat.* **197,** 216–235 (2021).
28. Filippou, C., Diss, R. M., Daudu, J. O., Coutts, R. H. A. & Kotta-Loizou, I. The Polymycovirus-Mediated Growth Enhancement of the Entomopathogenic Fungus *Beauveria bassiana* Is Dependent on Carbon and Nitrogen Metabolism. *Front. Microbiol.* **12,** 12 (2021).

29. Fisher, M. C., Pasmans, F. & Martel, A. Virulence and Pathogenicity of Chytrid Fungi Causing Amphibian Extinctions. *Annu. Rev. Microbiol.* **75,** 673–693 (2021).
30. Joneson, S., Stajich, J. E., Shiu, S.-H. & Rosenblum, E. B. Genomic transition to pathogenicity in chytrid fungi. *PLoS Pathog.* **7,** e1002338 (2011).
31. Krupovic, M. & Forterre, P. Single-stranded DNA viruses employ a variety of mechanisms for integration into host genomes. *Ann. N. Y. Acad. Sci.* **1341,** 41–53 (2015).
32. Choi, G. H. & Nuss, D. L. Hypovirulence of chestnut blight fungus conferred by an infectious viral cDNA. *Science* **257,** 800–803 (1992).
33. Filloux, D., Murrell, S., Koohapitagtam, M., Golden, M., Julian, C., Galzi, S., Uzest, M., Rodier-Goud, M., D'Hont, A., Vernerey, M. S., Wilkin, P., Peterschmitt, M., Winter, S., Murrell, B., Martin, D. P. & Roumagnac, P. The genomes of many yam species contain transcriptionally active endogenous geminiviral sequences that may be functionally expressed. *Virus Evol* **1,** vev002 (2015).
34. Skirmuntt, E. C., Escalera-Zamudio, M., Teeling, E. C., Smith, A. & Katzourakis, A. The Potential Role of Endogenous Viral Elements in the Evolution of Bats as Reservoirs for Zoonotic Viruses. *Annu Rev Virol* **7,** 103–119 (2020).
35. Yu, X., Li, B., Fu, Y., Xie, J., Cheng, J., Ghabrial, S. A., Li, G., Yi, X. & Jiang, D. Extracellular transmission of a DNA mycovirus and its use as a natural fungicide. **110,** 1452–1457 (2013).
36. Myers, J. M. & James, T. Y. Mycoviruses. *Curr. Biol.* **32,** R150–R155 (2022).
37. Schloegel, L. M., Toledo, L. F., Longcore, J. E., Greenspan, S. E., Vieira, C. A., Lee, M., Zhao, S., Wangen, C., Ferreira, C. M., Hipolito, M., Davies, A. J., Cuomo, C. A., Daszak, P. & James, T. Y. Novel, panzootic and hybrid genotypes of amphibian chytridiomycosis associated with the bullfrog trade. *Mol. Ecol.* **21,** 5162–5177 (2012).
38. Greenspan, S. E., Lambertini, C., Carvalho, T., James, T. Y., Toledo, L. F., Haddad, C. F. B. & Becker, C. G. Hybrids of amphibian chytrid show high virulence in native hosts. *Sci.*

Rep. **8,** 9600 (2018).

39. Li, H. & Durbin, R. Fast and accurate long-read alignment with Burrows-Wheeler transform. *Bioinformatics* **26,** 589–595 (2010).
40. Prjibelski, A., Antipov, D., Meleshko, D., Lapidus, A. & Korobeynikov, A. Using SPAdes De Novo Assembler. *Curr. Protoc. Bioinformatics* **70,** e102 (2020).
41. Hyatt, D., Chen, G.-L., Locascio, P. F., Land, M. L., Larimer, F. W. & Hauser, L. J. Prodigal: prokaryotic gene recognition and translation initiation site identification. *BMC Bioinformatics* **11,** 119 (2010).
42. Edgar, R. C. Muscle5: High-accuracy alignment ensembles enable unbiased assessments of sequence homology and phylogeny. *Nat. Commun.* **13,** 6968 (2022).
43. Minh, B. Q., Schmidt, H. A., Chernomor, O., Schrempf, D., Woodhams, M. D., von Haeseler, A. & Lanfear, R. IQ-TREE 2: New Models and Efficient Methods for Phylogenetic Inference in the Genomic Era. *Mol. Biol. Evol.* **37,** 1530–1534 (2020).
44. Kamvar, Z. N., Tabima, J. F. & Grünwald, N. J. Poppr: an R package for genetic analysis of populations with clonal, partially clonal, and/or sexual reproduction. *PeerJ* **2,** e281 (2014).
45. Galili, T. dendextend: an R package for visualizing, adjusting and comparing trees of hierarchical clustering. *Bioinformatics* **31,** 3718–3720 (2015).
46. Bolger, A. M., Lohse, M. & Usadel, B. Trimmomatic: a flexible trimmer for Illumina sequence data. *Bioinformatics* **30,** 2114–2120 (2014).
47. Noé, L. & Kucherov, G. YASS: enhancing the sensitivity of DNA similarity search. *Nucleic Acids Res.* **33,** W540–3 (2005).
48. Wick, R. R., Schultz, M. B., Zobel, J. & Holt, K. E. Bandage: interactive visualization of de novo genome assemblies. *Bioinformatics* **31,** 3350–3352 (2015).
49. Carter-House, D., E Stajich, J., Unruh, S. & Kurbessoian, T. Fungal CTAB DNA Extraction v1. (2020). doi:10.17504/protocols.io.bhx8j7rw
50. Koren, S., Walenz, B. P., Berlin, K., Miller, J. R., Bergman, N. H. & Phillippy, A. M. Canu:

scalable and accurate long-read assembly via adaptive k-mer weighting and repeat separation. *Genome Res.* **27,** 722–736 (2017).

51. Walker, B. J., Abeel, T., Shea, T., Priest, M., Abouelliel, A., Sakthikumar, S., Cuomo, C. A., Zeng, Q., Wortman, J., Young, S. K. & Earl, A. M. Pilon: an integrated tool for comprehensive microbial variant detection and genome assembly improvement. *PLoS One* **9,** e112963 (2014).
52. Palmer, J. M. & Stajich, J. *Funannotate v1.8.1: Eukaryotic genome annotation*. (Zenodo, 2020). doi:10.5281/ZENODO.1134477
53. Simmons, D. R., Bonds, A. E., Castillo, B. T., Clemons, R. A., Glasco, A. D., Myers, J. M., Thapa, N., Letcher, P. M., Powell, M. J., Longcore, J. E. & James, T. Y. The Collection of Zoosporic Eufungi at the University of Michigan (CZEUM): Introducing a new repository of barcoded Chytridiomyceta and Blastocladiomycota cultures. *IMA Fungus* **11,** 20 (2020).
54. Jenkinson, T. S., Betancourt Román, C. M., Lambertini, C., Valencia-Aguilar, A., Rodriguez, D., Nunes-de-Almeida, C. H. L., Ruggeri, J., Belasen, A. M., da Silva Leite, D., Zamudio, K. R., Longcore, J. E., Toledo, F. L. & James, T. Y. Amphibian-killing chytrid in Brazil comprises both locally endemic and globally expanding populations. *Mol. Ecol.* **25,** 2978–2996 (2016).
55. Schindelin, J., Arganda-Carreras, I., Frise, E., Kaynig, V., Longair, M., Pietzsch, T., Preibisch, S., Rueden, C., Saalfeld, S., Schmid, B., Tinevez, J.-Y., White, D. J., Hartenstein, V., Eliceiri, K., Tomancak, P. & Cardona, A. Fiji: an open-source platform for biological-image analysis. *Nat. Methods* **9,** 676–682 (2012).
56. Brewster, J. D. A simple micro-growth assay for enumerating bacteria. *J. Microbiol. Methods* **53,** 77–86 (2003).
57. Warringer, J. & Blomberg, A. Automated screening in environmental arrays allows analysis of quantitative phenotypic profiles in *Saccharomyces cerevisiae*. *Yeast* **20,** 53–67 (2003).
58. Jenkinson, T. S., Rodriguez, D., Clemons, R. A., Michelotti, L. A., Zamudio, K. R., Toledo,

L. F., Longcore, J. E. & James, T. Y. Globally invasive genotypes of the amphibian chytrid outcompete an enzootic lineage in coinfections. *Proc. Biol. Sci.* **285,** 20181894 (2018).

59. Boyle, D. G., Boyle, D. B., Olsen, V., Morgan, J. A. T. & Hyatt, A. D. Rapid quantitative detection of chytridiomycosis (*Batrachochytrium dendrobatidis*) in amphibian samples using real-time Taqman PCR assay. *Dis. Aquat. Organ.* **60,** 141–148 (2004).

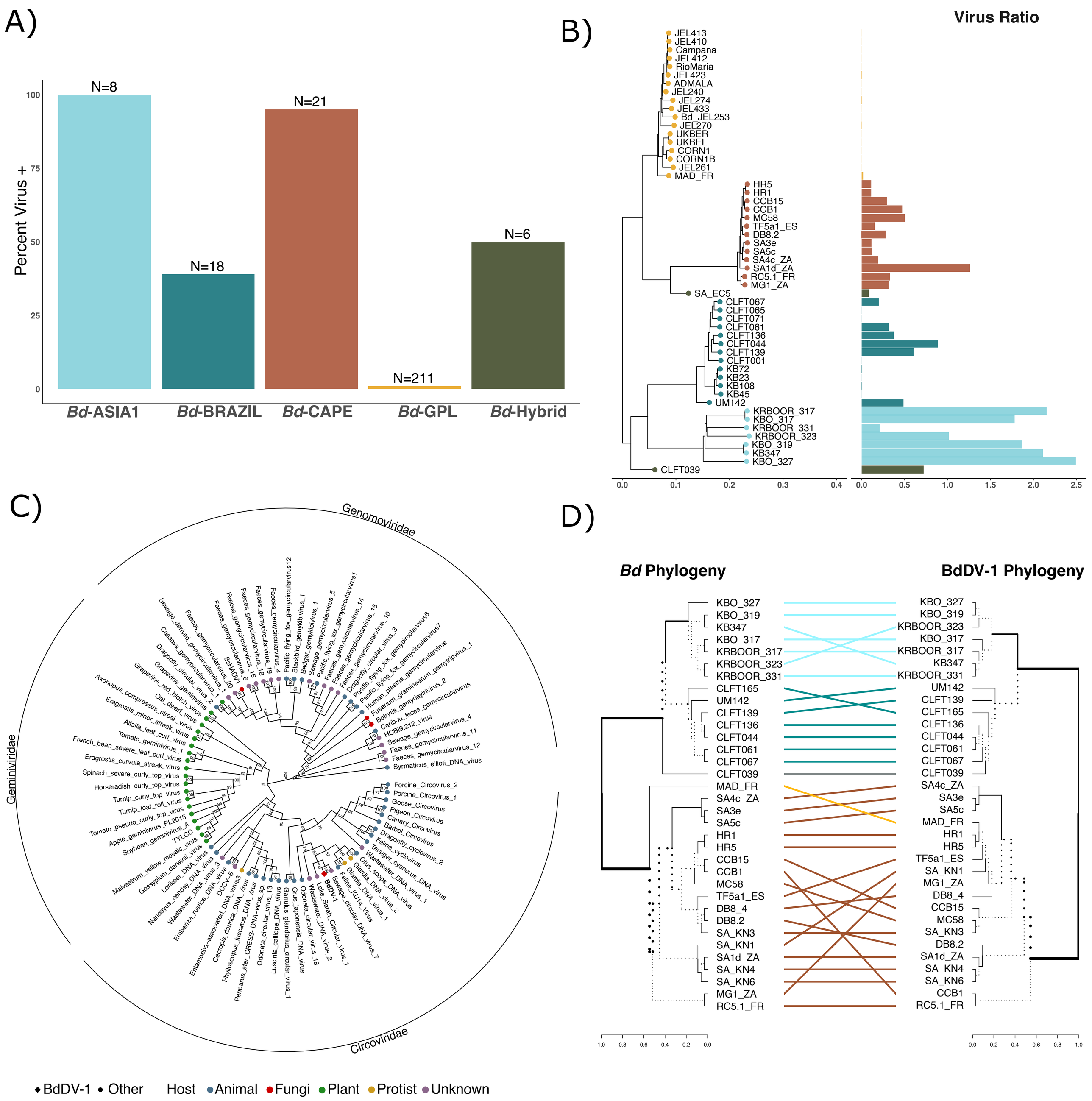
A)
Percent Virus +
N=8
N=18
N=21
N=211
N=6
Bd-ASIA1
Bd-BRAZIL
Bd-CAPE
Bd-GPL
Bd-Hybrid
B)
Virus Ratio
C)
Genomoviridae
Geminiviridae
Circoviridae
BdDV-1
D)
Bd Phylogeny
BdDV-1 Phylogeny
BdDV-1
Other
Host
Animal
Fungi
Plant
Protist
Unknown

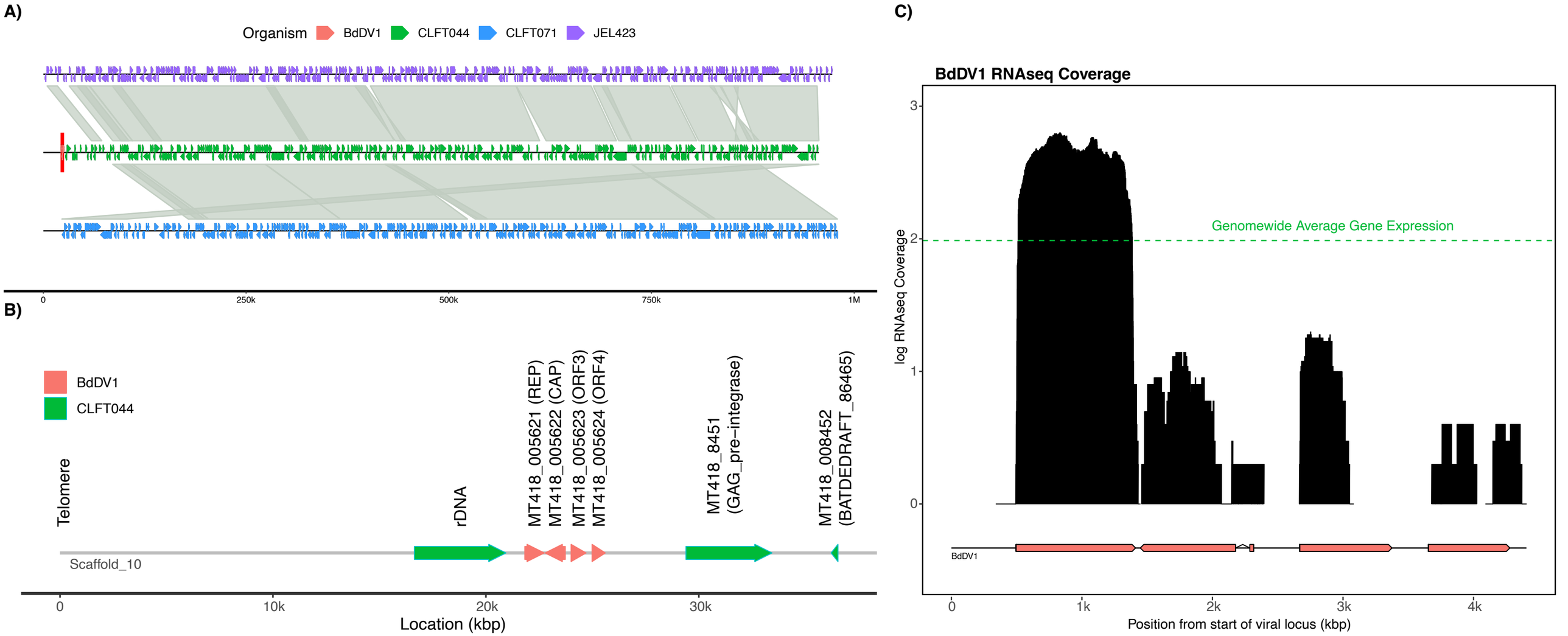
A)
Organism
BdDV1
CLFT044
CLFT071
JEL423
0
250k
500k
750k
1M
B)
BdDV1
CLFT044
Telomere
rDNA
MT418_005621 (REP)
MT418_005622 (CAP)
MT418_005623 (ORF3)
MT418_005624 (ORF4)
MT418_8451
(GAG_pre−integrase)
MT418_008452
(BATDEDRAFT_86465)
Scaffold_10
0
10k
20k
30k
Location (kbp)
C)
BdDV1 RNAseq Coverage
Genomewide Average Gene Expression
log RNAseq Coverage
3
2
1
0
BdDV1
0
1k
2k
3k
4k
Position from start of viral locus (kbp)

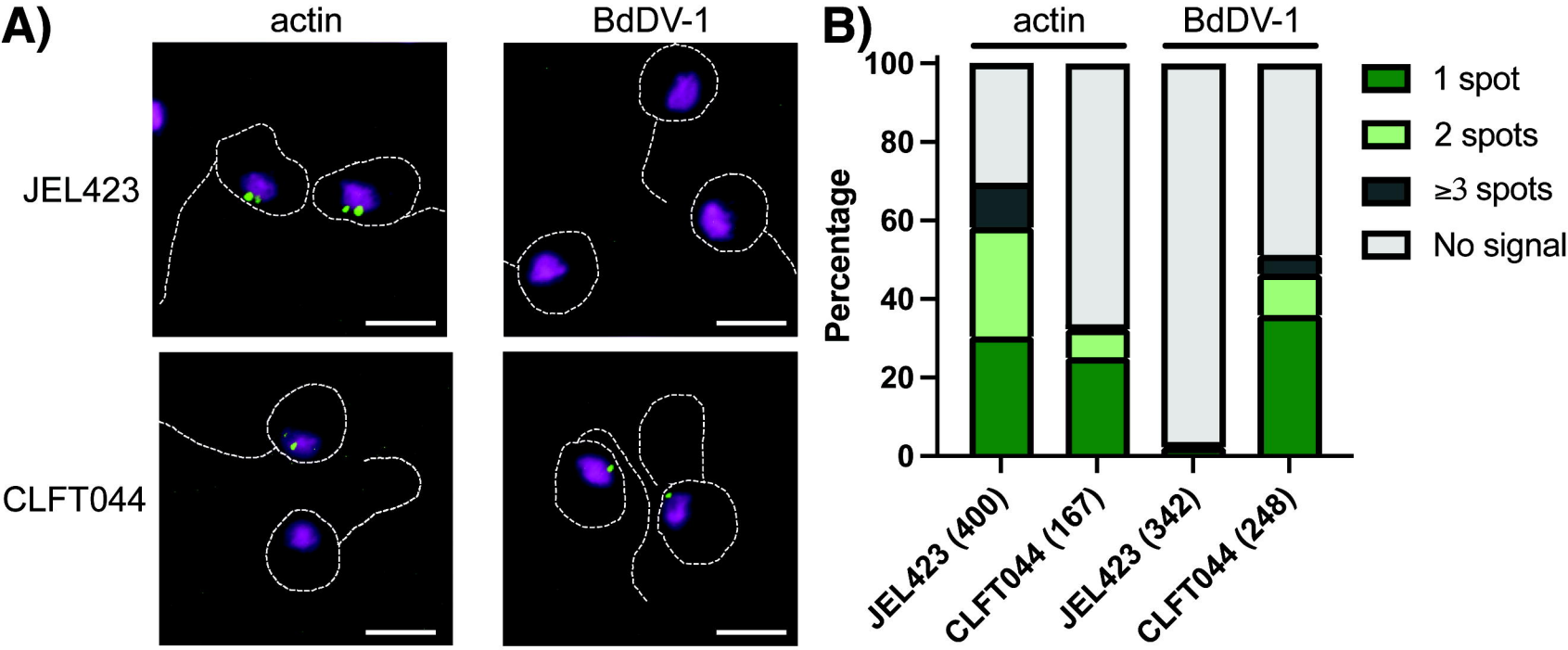
A)
actin
BdDV-1
JEL423
CLFT044
B)
actin
BdDV-1
Percentage
100
80
60
40
20
0
1 spot
2 spots
≥3 spots
No signal
JEL423 (400)
CLFT044 (167)
JEL423 (342)
CLFT044 (248)

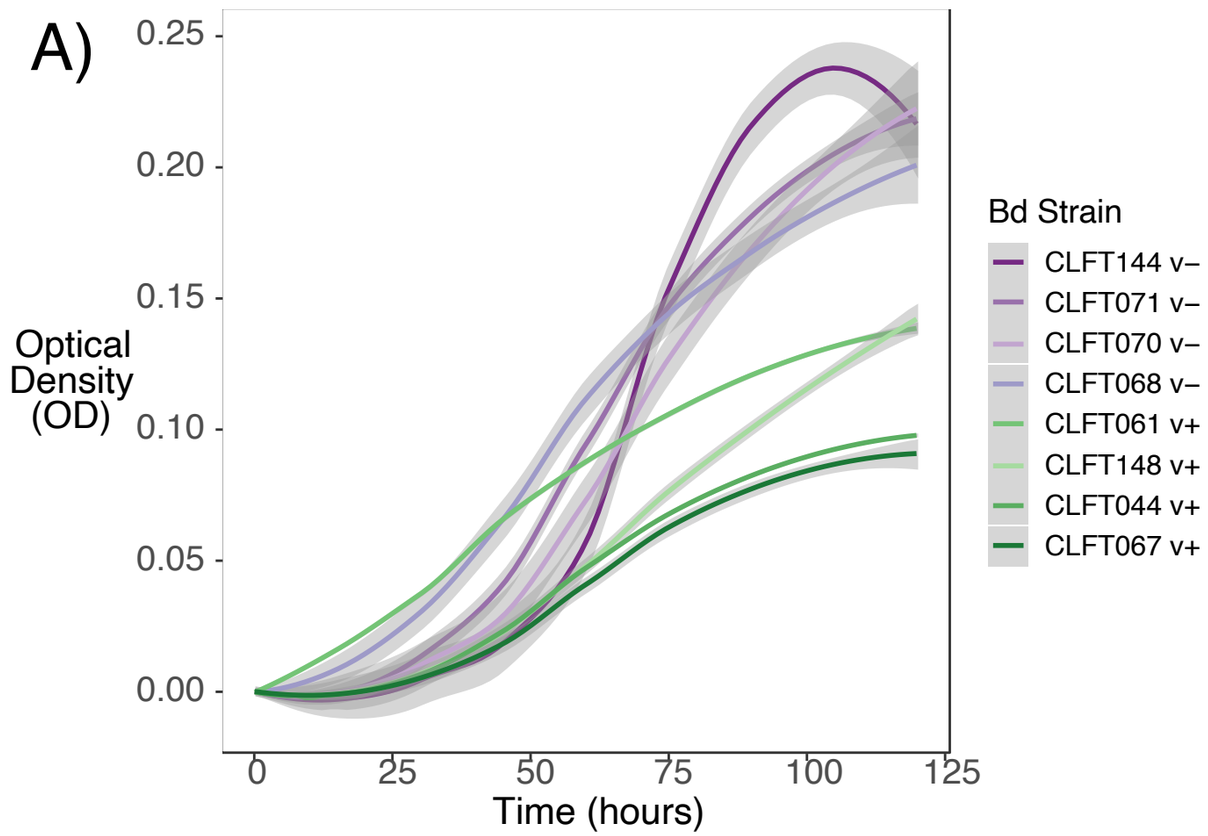
A)
0.25
0.20
0.15
0.10
0.05
0.00
Optical Density (OD)
0
25
50
75
100
125
Time (hours)
Bd Strain
CLFT144 v–
CLFT071 v–
CLFT070 v–
CLFT068 v–
CLFT061 v+
CLFT148 v+
CLFT044 v+
CLFT067 v+

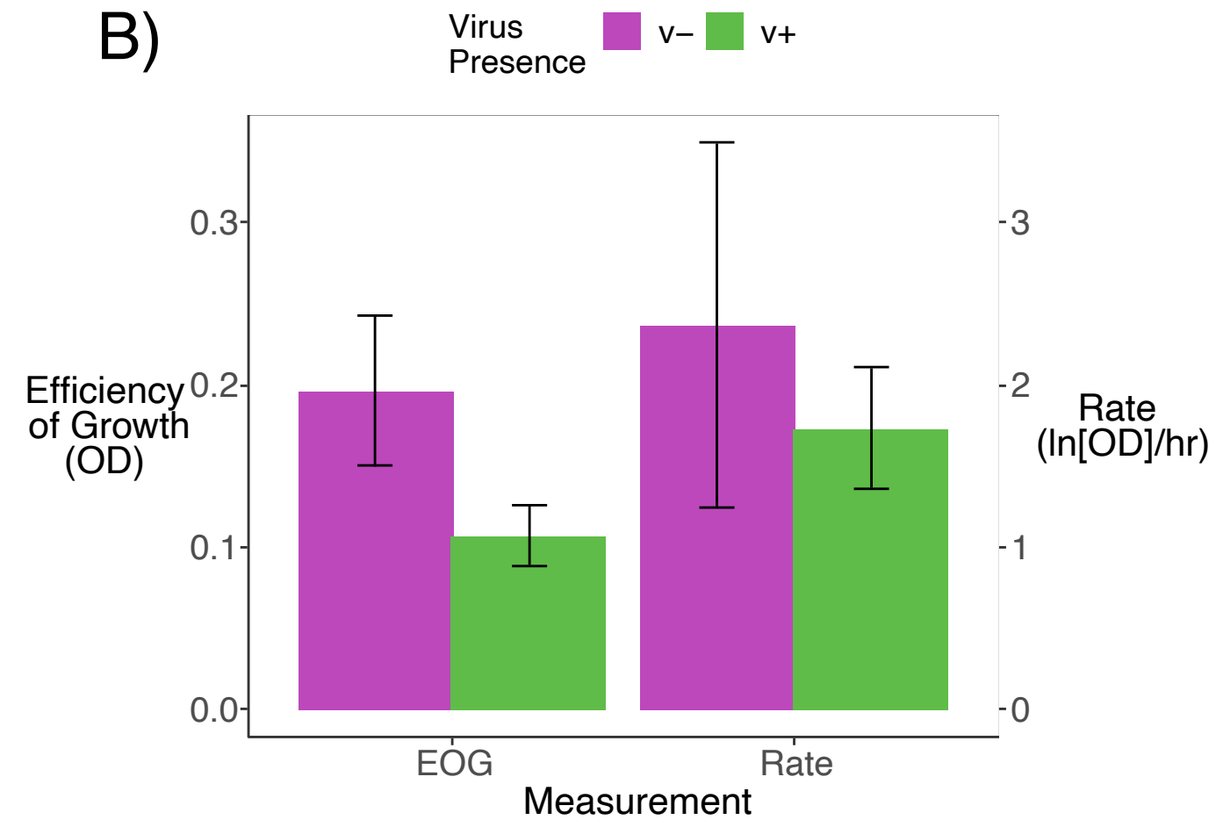
B)
Virus Presence
v–
v+
0.3
0.2
0.1
0.0
Efficiency of Growth (OD)
3
2
1
0
Rate (ln[OD]/hr)
EOG
Rate
Measurement

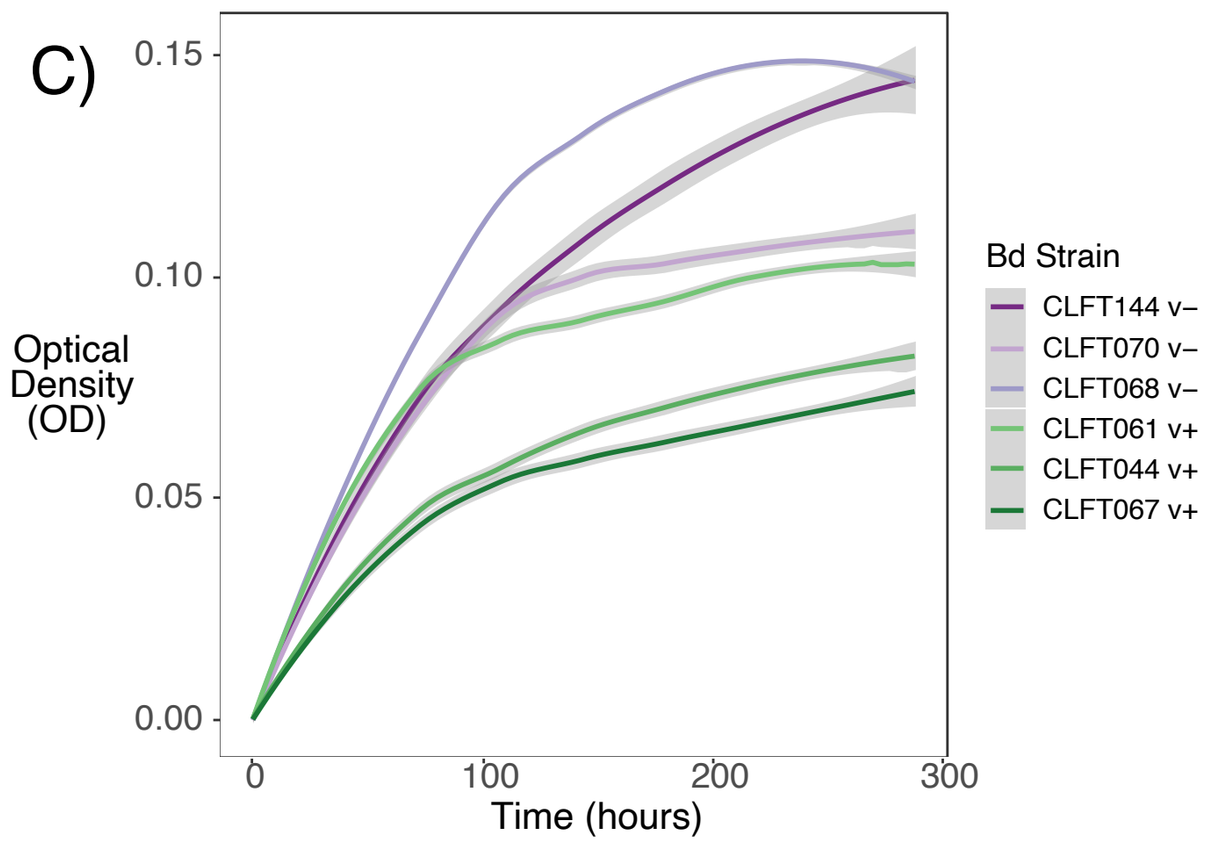
C)
0.15
0.10
0.05
0.00
Optical Density (OD)
0
100
200
300
Time (hours)
Bd Strain
CLFT144 v–
CLFT070 v–
CLFT068 v–
CLFT061 v+
CLFT044 v+
CLFT067 v+

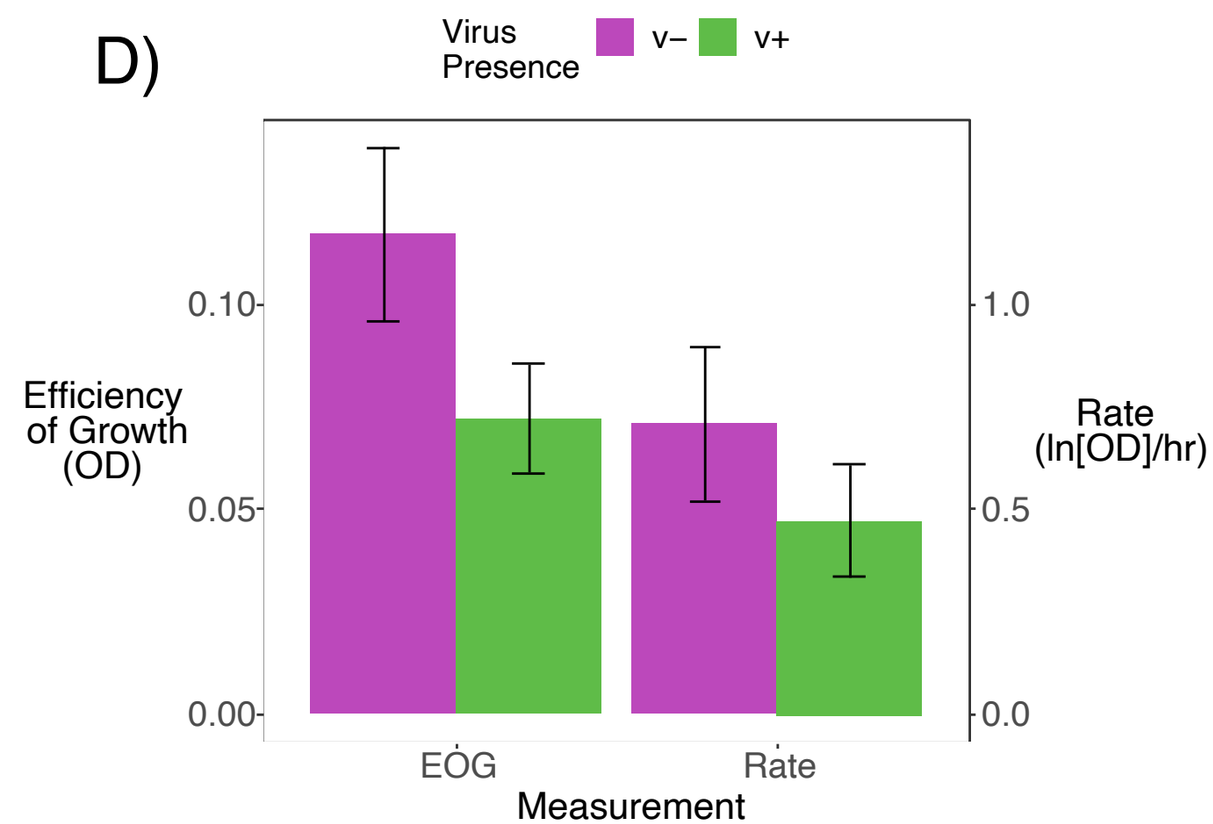
D)
Virus Presence
v–
v+
0.10
0.05
0.00
Efficiency of Growth (OD)
1.0
0.5
0.0
Rate (ln[OD]/hr)
EOG
Rate
Measurement

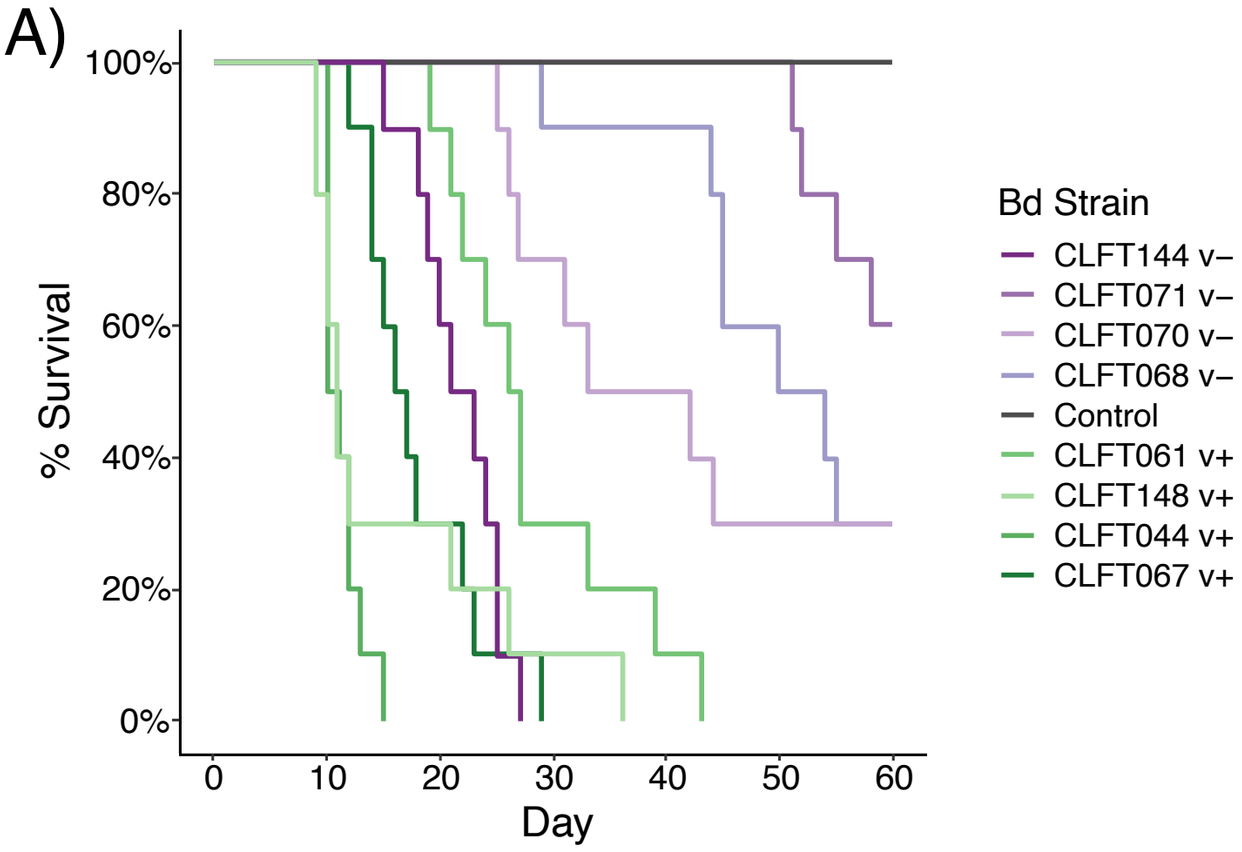
A)
100%
80%
60%
40%
20%
0%
% Survival
0
10
20
30
40
50
60
Day
Bd Strain
CLFT144 v–
CLFT071 v–
CLFT070 v–
CLFT068 v–
Control
CLFT061 v+
CLFT148 v+
CLFT044 v+
CLFT067 v+

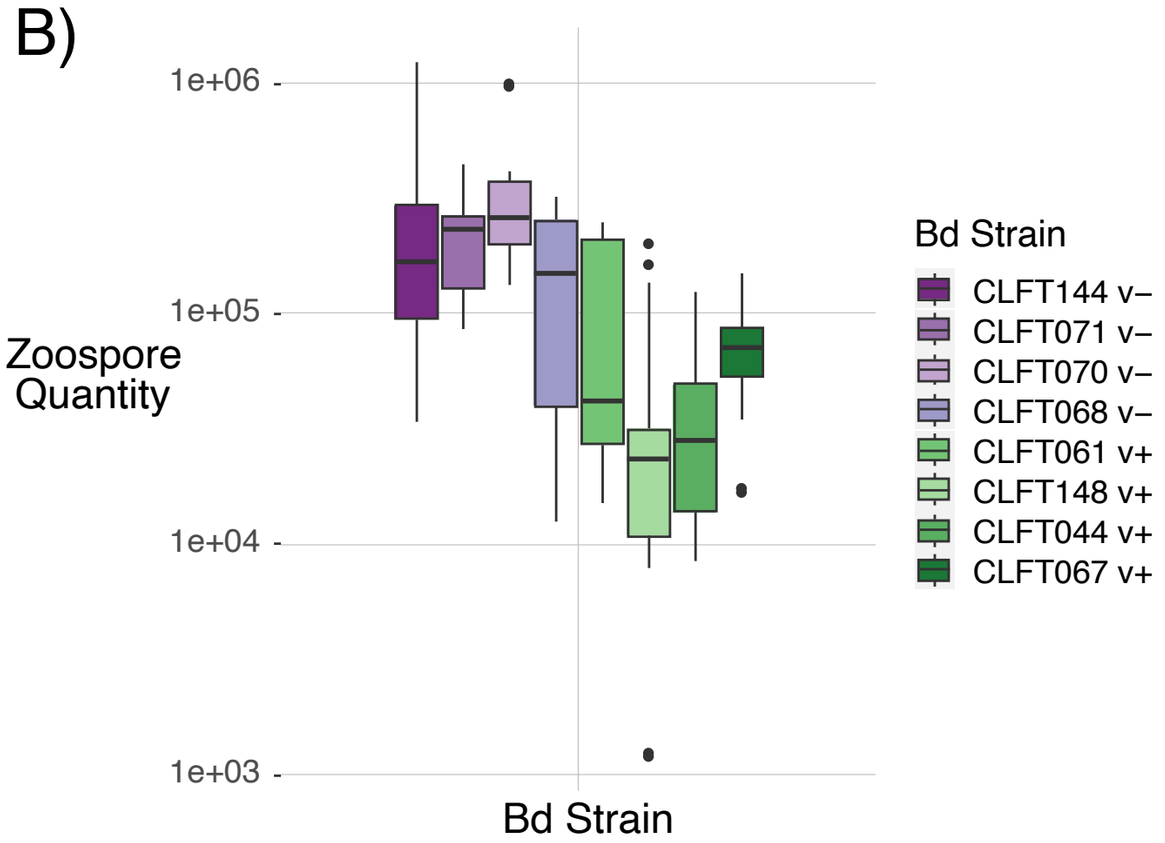
B)
1e+06
1e+05
1e+04
1e+03
Zoospore Quantity
Bd Strain
Bd Strain
CLFT144 v–
CLFT071 v–
CLFT070 v–
CLFT068 v–
CLFT061 v+
CLFT148 v+
CLFT044 v+
CLFT067 v+